

Active Control Vibration of a Smart Composite Plate for various Boundary Conditions

Dr.M. Latrache ¹, N.Menasri ²

¹Associate Professor, University Mohamed Boudiaf M'sila, B.P 166 ICHBELIA .M'sila 28000, Algeria.

²Associate Professor ,Laboratoire de Matériaux et Mécanique des Structures (LMMS), Université Mohamed Boudiaf M'sila. Algérie.

Abstract: In this paper, the finite element formulation of the classical laminated plate with embedded piezoelectric patches is based on the first order shear deformation theory (FSDT) and Hamilton's principle, in this formulation the mass and stiffness of the piezoelectric have been taken into account. The formulation results in a coupled finite element model with mechanical (displacements) and electrical (charges at electrodes) degrees of freedom. The use of the piezoelectric actuator and sensor patches for vibration active control of smart composite plates is discussed. A Linear Quadratic Regulator (LQR) controller is designed based on the independent mode space control techniques to stifle the vibration of the system. Numerical results obtained with the present finite element FE model are found to be in good agreement with ANSYS. The effects of the boundary conditions control vibration of the smart composite plate are examined.

Keywords: Piezoelectric, smart composite plate, finite element, Active control, LQR

1. Introduction

In the recent years, piezoelectric materials have been studied extensively for use as smart structures(Cao, Tanner, & Chronopoulos, 2020; Chandrashekhara & Agarwal, 1993; Hasheminejad & Oveisi, 2016; Lee & Moon, 1990; Roy & Chakraborty, 2009; Sohn, Choi, & Kim, 2011; Wankhade & Bajoria, 2021). A smart structure can be defined as a structure or structural component with bonded or embedded sensors and actuators as well as control systems, which change the shape and dynamic behavior of the structure. Smart structures and systems have self-inspection and inherent adaptive capabilities. They can respond almost instantaneously to the changes in the external environment and hence can greatly enhance the performance of existing structures. The research and implementation of smart structures and systems opens new opportunities for radical changes in the design of adaptive structures and high performance structures(G. Liu, Peng, Lam, & Tani, 1999).

Elements have also become available in commercial finite element codes such as ANSYS (Documentation, 2011) and ABAQUS. On the other hand, the design of smart structures is multidisciplinary by nature. Design of a smart structure system requires more than accurate structural modeling. To design piezoelectric smart structures for active vibration control, both structural dynamics and control theory need be considered.

An active vibration control using smart material is being increasingly used for flexible structures in aerospace industry. Over the last decade the usage of piezoelectric as actuators and sensors has considerably increased and they provide effective means of high quality actuation and sensing mechanism. Time lag, signal conditioning, placement and bonding issues are very easy to resolve with piezoelectric(Sethi & Song, 2004).

Great efforts were devoted to studying the vibrations of constrained piezoelectric composite damping plates. Reddy (Junuthula N Reddy, 1984) and Mallek *et al* (Mallek, Jrad, Wali, & Dammak, 2021) who presented the formulation of a finite element model for the analysis of general laminate composite plate. The displacement field is based in a first order shear deformation theory (FSDT). this theory has been considered to designate the electromechanical state of the piezoelectric patches bonded on an elastic composite plate.

Chhabra *et al* (Chhabra, Bhushan, & Chandna, 2016) and Liu (X. Liu, Cai, Peng, & Zhang, 2018) studied the optimal placement of piezoelectric actuators on a thin plate using the integer-coded genetic algorithm. Jia *et al* (Jia, He, & Zhang, 2020) studied the effect of linear quadratic regulator (LQR) for vibration reduction. Abdelrahman *et al* (Abdelrahman, Al-Garni, Abdelmaksoud, & Abdallah, 2018) developed numerical technique to study the Effect of Piezoelectric Patch Size and Material on Active Vibration Control of Wind Turbine Blades. The simulation results show that LQR controller produces considerable reduction in both the settling time and the actuation force. Quek *et al* (Quek, Wang, & Ang, 2003) studied a simple optimal placement strategy of piezoelectric actuator/sensor pairs on a laminated composite plate and employed the classical direct pattern search method to obtain the local optimum. Han and Lee (Han & Lee, 1999) studied the optimal placement of piezoelectric actuators and sensors on a composite plate, where the locations of both sensors and actuators were determined with consideration of controllability, observability and spillover prevention

Kumar (Kumar & Narayanan, 2007) and Sadri *et al* (Sadri, Wright, & Wynne, 1999) studied the optimal placement of collocated piezoelectric actuator/sensor pairs on a thin plate using the model-based linear quadratic regulator (LQR) controller, where the LQR performance was taken as the optimization criterion and GA was taken as the optimization algorithm. Jandaghian *et al* (Jandaghian, Jafari, & Rahmani, 2014) studied the harmonic forced vibration of circular functionally graded plate integrated with two uniformly distributed actuator faces made of piezoelectric material .The results show that thickness of piezoelectric layer and changing the power index in FG material has a significant influence on the deflection and natural frequencies of system.

The paper is organized as follows. In section 2 the finite element FE formulation of a composite plate embedded with piezoelectric patches, sections 3 are presented the active vibration control procedure and LQR problem; the numerical analysis validation of literature Liu(G. Liu et al., 1999) and effects of boundary conditions for active vibration control are described in detail in section 4. Finally, conclusions are drawn in Section 5.

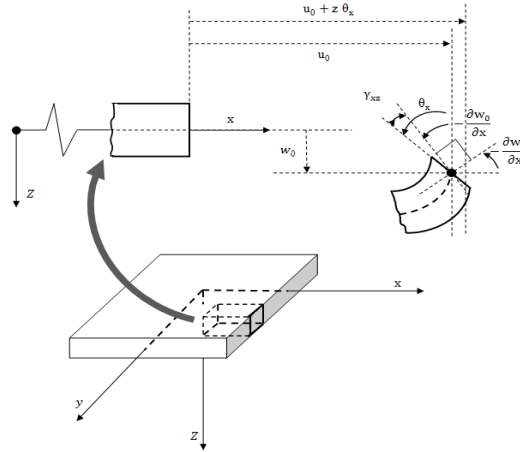
2. Finite element model

The enormous numbers of publications are widely presented and discussed the mathematical aspects of a general finite element (FE) statement of laminate composite plate with embedded piezoelectric patches problems (Kapuria & Yasin, 2010; Karegar, Bidgoli, & Mazaheri, 2021; Junuthula Narasimha Reddy, 2003).

2.1 Mechanical displacements and strains

In the present study first Shear deformation laminated plate theory used is discussed as follows. In the first-order shear deformation laminated plate theory (FSDT).

Figure.1.The assumptions for the first order shear deformation theory



The displacement fields for the laminate plate (figure.1), are proposed by (Malgaca, 2010; Mallek et al., 2021; Junuthula N Reddy, 1984).

$$\begin{cases} U_1(x, y, z, t) = u_0(x, y, t) + z\theta_x(x, y, t) \\ U_2(x, y, z, t) = v_0(x, y, t) + z\theta_y(x, y, t) \\ U_3(x, y, z, t) = w_0(x, y, t) \end{cases} \quad (1)$$

The deformation field related with the displacement field by:

$$\{\varepsilon\} = \{\varepsilon_{xx} \varepsilon_{yy} \varepsilon_{xy}\}^T = \varepsilon_0 + z\kappa \quad (2)$$

With:

$$\begin{Bmatrix} \varepsilon_{x0} \\ \varepsilon_{y0} \\ \varepsilon_{z0} \end{Bmatrix} = \begin{bmatrix} \frac{\partial u_0}{\partial x} \\ \frac{\partial v_0}{\partial y} \\ \frac{\partial u_0}{\partial y} + \frac{\partial v_0}{\partial x} \end{bmatrix} \quad (3)$$

And:

$$\begin{Bmatrix} K_x \\ K_y \\ K_{xy} \end{Bmatrix} = \begin{bmatrix} \frac{\partial \theta_x}{\partial x} \\ \frac{\partial \theta_y}{\partial y} \\ \frac{\partial \theta_x}{\partial y} + \frac{\partial \theta_y}{\partial x} \end{bmatrix} \quad (4)$$

Thereafter:

$$\{\varepsilon\} = [L]\{U\} \quad (5)$$

Where [L] :

$$[L] = \begin{bmatrix} \frac{\partial}{\partial x} & 0 & 0 & 0 & 0 \\ 0 & \frac{\partial}{\partial y} & 0 & 0 & 0 \\ 0 & 0 & \frac{\partial}{\partial y} & 0 & 1 \\ 0 & 0 & \frac{\partial}{\partial x} & 1 & 0 \\ \frac{\partial}{\partial y} & \frac{\partial}{\partial x} & 0 & 0 & 0 \\ 0 & 0 & 0 & \frac{\partial}{\partial x} & 0 \\ 0 & 0 & 0 & 0 & \frac{\partial}{\partial y} \\ 0 & 0 & 0 & \frac{\partial}{\partial y} & \frac{\partial}{\partial x} \end{bmatrix} \quad (6)$$

The transverse shear deformations are assumed by:

$$\gamma = \begin{Bmatrix} \gamma_{yz} \\ \gamma_{xz} \end{Bmatrix} = \begin{bmatrix} \frac{\partial w_0}{\partial y} + \theta_y \\ \frac{\partial w_0}{\partial x} + \theta_x \end{bmatrix} \quad (7)$$

The coefficients $Q_{ij}^{(k)}$ are known in terms engineering constants of the kth layer:

$$Q_{11}^{(k)} = \frac{E_1^{(k)}}{1 - \nu_{12}^{(k)} \nu_{21}^{(k)}} \quad (8)$$

$$Q_{12}^{(k)} = \frac{\nu_{12}^{(k)} E_2^{(k)}}{1 - \nu_{12}^{(k)} \nu_{21}^{(k)}} \quad (9)$$

$$Q_{22}^{(k)} = \frac{E_2^{(k)}}{1 - \nu_{12}^{(k)} \nu_{21}^{(k)}} \quad (10)$$

$$Q_{66}^{(k)} = G_{12}^{(k)} \quad (11)$$

$$Q_{55}^{(k)} = G_{13}^{(k)} \quad (12)$$

$$Q_{44}^{(k)} = G_{23}^{(k)} \quad (13)$$

Where:

E_1, E_2 : Are the two Young's module in the x and y directions.

G_{12}, G_{13} and G_{23} : Are the shear modules.

ν_{12}, ν_{21} : Are the Poisson coefficients.

The stresses-strains in each layer of a laminate composite plate are given by:

$$\begin{bmatrix} \sigma_{xx} \\ \sigma_{yy} \\ \tau_{xy} \\ \tau_{xz} \\ \tau_{yz} \end{bmatrix}^{(k)} = \begin{bmatrix} \bar{Q}_{11} & \bar{Q}_{12} & \bar{Q}_{16} & 0 & 0 \\ \bar{Q}_{21} & \bar{Q}_{22} & \bar{Q}_{26} & 0 & 0 \\ \bar{Q}_{61} & \bar{Q}_{62} & \bar{Q}_{66} & 0 & 0 \\ 0 & 0 & 0 & k_s \bar{Q}_{55} & k_s \bar{Q}_{54} \\ 0 & 0 & 0 & k_s \bar{Q}_{45} & k_s \bar{Q}_{44} \end{bmatrix}^{(k)} \begin{bmatrix} \varepsilon_{xx} \\ \varepsilon_{yy} \\ \gamma_{xy} \\ \gamma_{xz} \\ \gamma_{yz} \end{bmatrix}^{(k)} \quad (14)$$

Where:

k_s : Is the shear correction factor

And:

$$[\bar{Q}_{ij}] = [T]^T [Q_{ij}^{(k)}] [T] \quad (15)$$

Where:

[T] : Is a transformation matrix

$$[T] = \begin{bmatrix} \cos^2 \Phi & \sin^2 \Phi & -\sin 2\Phi & 0 & 0 \\ \sin^2 \Phi & \cos^2 \Phi & \sin 2\Phi & 0 & 0 \\ \sin \Phi \cos \Phi & -\sin \Phi \cos \Phi & \cos^2 \Phi - \sin^2 \Phi & 0 & 0 \\ 0 & 0 & 0 & \cos \Phi & \sin \Phi \\ 0 & 0 & 0 & -\sin \Phi & \cos \Phi \end{bmatrix} \quad (16)$$

The equations of the resulting stresses are obtained as follows:

$$\{\bar{N}\} = [\bar{D}]\{\varepsilon\} - \{\bar{N}^E\} \quad (17)$$

With:

$$\{\bar{N}\} = (N_x, N_y, Q_y, Q_x, N_{xy}, M_x, M_y, M_{xy})^T \quad (18)$$

$$(N_x, M_x) = \int_{-\frac{h}{2}}^{\frac{h}{2}} \sigma_x(1, z) dz \quad (19)$$

$$(N_y, M_y) = \int_{-\frac{h}{2}}^{\frac{h}{2}} \sigma_y(1, z) dz \quad (20)$$

$$(N_{xy}, M_{xy}) = \int_{-\frac{h}{2}}^{\frac{h}{2}} \tau_{xy}(1, z) dz \quad (21)$$

$$Q_x = \int_{-\frac{h}{2}}^{\frac{h}{2}} \tau_{xz} dz \quad (22)$$

$$Q_y = \int_{-\frac{h}{2}}^{\frac{h}{2}} \tau_{yz} dz \quad (23)$$

Where:

[N]: tensor of the membrane resultants,

[Q]: vector of the resultants in shear, and

[M]: tensor of the moments of flexion-torsion.

The matrix $[\bar{D}]$ is defined by:

$$[\bar{D}] = \begin{bmatrix} A_{11} & A_{12} & 0 & 0 & A_{16} & B_{11} & B_{12} & B_{16} \\ A_{21} & A_{22} & 0 & 0 & A_{26} & B_{12} & B_{22} & B_{26} \\ 0 & 0 & A_{44} & A_{45} & 0 & 0 & 0 & 0 \\ 0 & 0 & A_{54} & A_{55} & 0 & 0 & 0 & 0 \\ A_{16} & A_{26} & 0 & 0 & A_{66} & B_{16} & B_{26} & B_{66} \\ B_{11} & B_{12} & 0 & 0 & B_{16} & D_{11} & D_{12} & D_{16} \\ B_{12} & B_{22} & 0 & 0 & B_{26} & D_{12} & D_{22} & D_{26} \\ B_{16} & B_{26} & 0 & 0 & B_{66} & D_{16} & D_{26} & D_{66} \end{bmatrix} \quad (24)$$

Where:

$[\bar{D}]$: tensor of generalized suppleness,

$[A_{ij}]$: matrix of membrane plate rigidities,

$[B_{ij}]$: matrix of membrane-flexion-torsion plate couplings, and

$[D_{ij}]$: matrix of the rigidities in flexion and torsion of plat.

We have the following relations:

$$A_{ij}, B_{ij}, D_{ij} = \sum_{k=1}^n \int_{z_k}^{z_{k+1}} [\bar{Q}_{ij}] (1, z, z^2) dz \quad (i, j = 1, 2, 6) \quad (25)$$

$$A_{ij} = \sum_{k=1}^n \int_{z_k}^{z_{k+1}} [\bar{Q}_{ij}] k_s dz \quad (i, j = 4, 5) \quad (26)$$

2.1 Piezoelectric constitutive equations

The piezoelectric effect can be expressed by four pairs of equations:

$$\begin{cases} \{\sigma\} = [Q]\{\varepsilon\} - [e]^T\{E\} \\ \{D\} = [e]\{\varepsilon\} - [\epsilon]\{E\} \end{cases} \quad (27)$$

Where:

$\{\varepsilon\}$: strain vector,

$\{\sigma\}$: stress vector,

$\{E\}$: vector of the electric field,

$\{D\}$: vector of electrical displacement,

$[Q]$: elasticity matrix at constant electric field,

$[e]$: piezoelectric constants matrix, and

$[\epsilon]$: dielectric matrix at constant strain.

The matrices $[e]$ and $[\epsilon]$ are expressed as:

$$[e] = \begin{bmatrix} 0 & 0 & e_{31} \\ 0 & 0 & e_{32} \\ 0 & 0 & 0 \\ 0 & e_{24} & 0 \\ e_{15} & 0 & 0 \end{bmatrix} \quad (28)$$

$$[\epsilon] = \begin{bmatrix} \epsilon_1 & 0 & 0 \\ 0 & \epsilon_2 & 0 \\ 0 & 0 & \epsilon_3 \end{bmatrix} \quad (29)$$

The electric field vector $\{E\}$ is given by:

$$E_x = -\frac{\partial \phi}{\partial x} \quad (31)$$

$$E_y = -\frac{\partial \phi}{\partial y} \quad (32)$$

$$E_z = -\frac{\partial \phi}{\partial z} \quad (33)$$

Where:

E_x , E_y and E_z : Are the component of the electric field in the x, y and z directions.

ϕ : Is the electrical potential:

Assuming that the distribution of the electric potential field $\{E\}$ varies linearly across the thickness of a piezoelectric element, and the voltage difference across its thickness is constant over its entire area.

The matrix $\{E\}$ can be expressed as:

$$\{E\} = \frac{1}{h_p} [0 \quad 0 \quad -1]^T \{\Delta \phi\} \quad (34)$$

Consequently, considering that:

$$E_z = -\frac{V^+}{h_p} \quad (35)$$

Where V^+ represents the electrical voltage at the terminals of the piezoelectric element is given by:

$$V^+ = \phi(h + h_p) - \phi(h) \quad (36)$$

Where h_p is the thickness of the piezoelectric element.

2.2 Hamilton principle

For a continuous system, the Hamilton principle is written between two instants t_1 and t_2 :

$$\int_{t_1}^{t_2} \delta(T - \psi + W) dt \quad (37)$$

Where:

- The kinetic energy:

$$T = \int_v \frac{1}{2} \rho \{\dot{U}\}^T \{\dot{U}\} dv \quad (38)$$

- The potential energy:

$$\psi = \int_v \frac{1}{2} (\{\varepsilon\}^T \{\sigma\} - \{E\}^T \{D\}) dv \quad (39)$$

- The work done by a force P_s :

$$W = \int_s \{\delta U\}^T \{P_s\} ds \quad (40)$$

Finally, the dynamic equations are done by:

$$\begin{cases} [M]\{\ddot{U}\} + [C]\{\dot{U}\} + [K]\{U\} + \{K_{me}\}\{\varphi\}_a + \{K_{me}\}\{\varphi^e\}_s = \{F_m\} \\ [K_{me}]_a^T \{u\} - [K_e]_a \{\varphi\}_a = -[K_e]_a \{\varphi\}_a \\ [K_{me}]_s^T \{u\} - [K_e]_s \{\varphi\}_s = -[K_e]_s \{\varphi\}_s \end{cases} \quad (41)$$

Where: [M], [C] and [K]: Are a matrix of masses, damping and stiffness respectively of the smart composite plate (composite plate + patches piezoelectric).

$[K_{me}]_a^T, [K_e]_a, [K_{me}]_s^T, [K_e]_s$: Are an electro-mechanic coupling and stiffness electric for actuator an sensor respectively.

$\{F_m\}$: Is vector of exterior force generalities.

3. Active vibration control

the characteristic equation for free vibration is

$$([K] - \omega_n^2 [M])\{U\} = 0 \quad (42)$$

With:

$$\{U\} = \sum_k^{N_{mode}} \{\Omega_k\} \{x(t)\} \quad (43)$$

Where:

$\{\Omega_k\}$: Is a Kth vibration mode of the smart plate.

$\{x(t)\}$: Is a modal contribution of the K mode.

$$\begin{aligned} [\Omega]^T [M] [\Omega] &= \text{diag}(\mu_k) \\ [\Omega]^T [K] [\Omega] &= \text{diag}(\mu_k \omega_k^2) \\ [\Omega]^T [C] [\Omega] &= \text{diag}(2\xi_k \omega_k^2) \end{aligned} \quad (44)$$

$$\begin{Bmatrix} \dot{x} \\ \ddot{x} \end{Bmatrix} = \begin{bmatrix} 0 & I \\ -\text{diag}(\omega_k^2) & -2\xi_k \omega_k \end{bmatrix} \begin{Bmatrix} x \\ \dot{x} \end{Bmatrix} - \begin{bmatrix} 0 \\ \mu \Omega^T K^{(i)}_{me} \end{bmatrix} \{\varphi^{(ac)}\} \quad (45)$$

Where [A], [B] and [C] denotethe system matrix, the input matrix and the system output matrix, respectively. They can be obtained as.

$$A = \begin{bmatrix} 0 & I \\ -\text{diag}(\omega_k^2) & -2\xi_k \omega_k \end{bmatrix} \quad (46)$$

$$B = \begin{bmatrix} 0 \\ \mu \Omega^T K^{(ac)}_{me} \end{bmatrix} \quad (47)$$

$$C = [K^{(i)}_{me} \quad \Omega \quad 0] \quad (48)$$

3.1. Objective function

To design such a Linear Quadratic Regulator LQR compensator, first, we consider the minimization of the quadratic cost function as follows:

$$J = \int_0^\infty (\{X\}^T [Q] \{X\} + \{\varphi\}^T [R] \{\varphi\}) dt = \min \quad (49)$$

Where:

Q Is a positive semidefinite matrix and R is a positive matrix.

The selection of Q and R is vital in the control design process. Q and R are the free parameters of design and stipulate the relative importance of the control result and the control effort. A large Q puts higher demands on control result, and a large R puts more limits on control effort (Schulz, Gomes, & Awruch, 2013).

The optimal solution is:

$$[G] = [R]^T [B]^T [K] \quad (50)$$

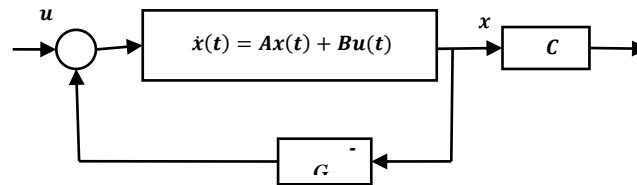
Where [K] satisfies the Riccati equation:

$$[A]^T [K] + [K] [A] - [K] [B] [R]^{-1} [B]^T [K] + [Q] = 0 \quad (51)$$

3.1 Linear Quadratic Regulator (LQR) problem

The state feedback approach can provide a complete model of the global response of the system under control. They are particularly applicable to the control of the first few modes of a structure. The state feedback (Fig.2) approach provides the best performance that can be achieved under an ideal feedback control system (Biglar, Gromada, Stachowicz, & Trzepieciński, 2015; Tian, Guo, & Shi, 2020).

Figure.2. The principle of the state feedback



In MATLAB, the command **lqr** is used to calculate the optimal gain matrix **G**.

Syntax: $[G, K, e] = \text{lqr}(A, B, Q, R)$

Where **e** is the closed-loop eigenvalues.

$$e = \text{eig}(A - BG) \quad (52)$$

4. Numerical analysis and discussions

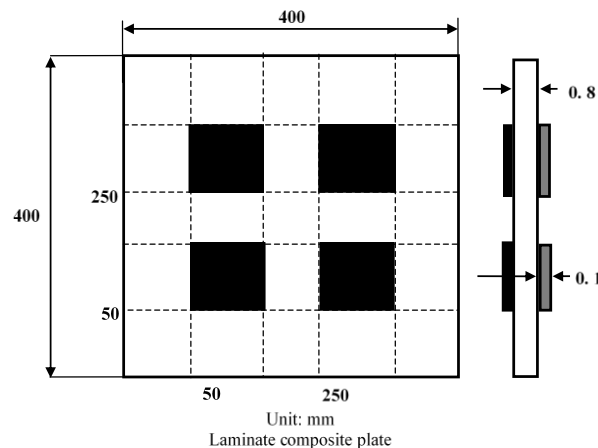
The numerical examples considered in the paper are chosen in correspondence with the existing numerical solutions that are available in the literature. The proposed finite element model was implemented in Matlab.

In this section, eigenfrequency results obtained with the proposed model are compared to results obtained by ANSYS APDL code and numerical results found in the open literature.

4.1 Validation

In this case, a square laminate plate composed of four layers of Graphite-Epoxy material $[-30/30/-30/30]$ (Figure.3). Covered by PZT G-1195 piezoelectric patches poled in z-direction (through-thickness) is considered.

Figure.3. The smart composite plate (G. Liu et al., 1999)



Case studies is presented in this section to demonstrate the validity of the literature.

Selected piezoelectric smart structure systems for active vibration control are designed using a finite element code ANSYS (ANSYS 2021 R1) and output feedback control law.

Three-dimensional coupled-field solid element (Solid 5) (Figure. 4) with 4 degree of freedom and 8 nodes is utilized to model piezoelectric patches, and three-dimensional structural multilayered solid element (Solid 186) (Figure. 5) with 3 degree of freedom and 20 nodes is employed to model host structures.

Figure.4. Solid5 geometry

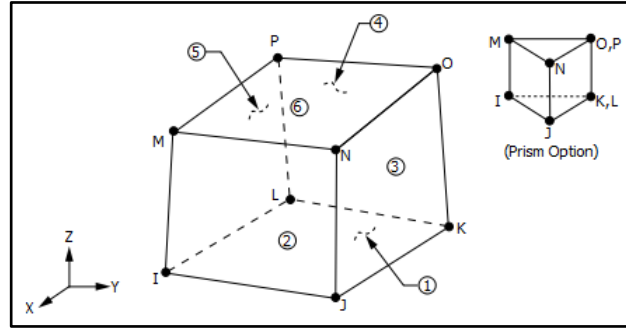
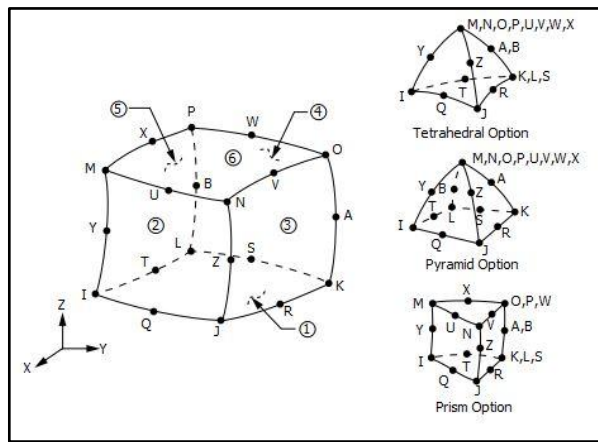


Figure.5. Solid 186 geometry



The material properties data for the composite plate, piezoelectric patches are given in table 1.

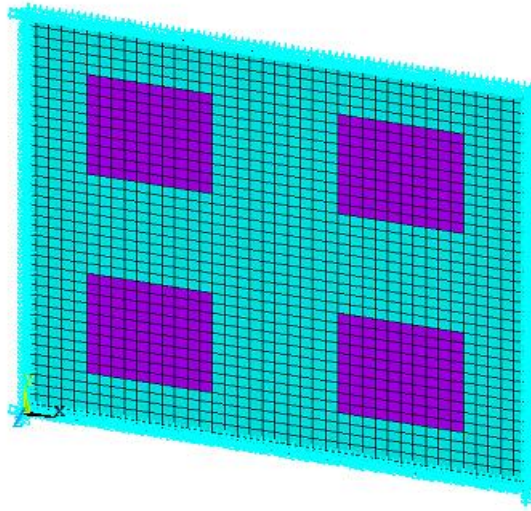
Table 1. The material properties data for the composite plate and piezoelectric patches.

properties	Graphite/epoxy	PZT G-1195
Poisson's ratio	0.31	0.3
Density ρ (kg/m³)	1550	7600
Elastic stiffness matrix (GPa)		
E11	119	132.38
E22	8.67	10.76
E33	8.67	10.76
G12	5.18	3.61
G13	3.29	5.61
G23	3.29	5.61
Piezoelectric constant (C/m²)		
e31	-	12.5
e33		12.5
e15		12.5
Dielectric constant (F/m)		
g11		1.53×10^{-8}
g22		1.53×10^{-8}
g33		1.53×10^{-8}

The FE model and the boundary conditions for simply supported plate shown in Figure 6, the FE model includes the composite plate, and a 4 pair of squares PZT actuators and sensors attached to the top and bottom surfaces of the plate.

The processing of the geometry and finite element mesh generation is provided by ANSYS processing analysis. The current structure is meshed by 40x40 eight-node solid elements, with 40 elements in width direction and 40 elements in the width direction. And each sensor and actuator are meshed with 100 identical elements. The simulation denotes the mechanical response of the plate equipped with the piezoelectric actuators without control.

Figure.6. Finite element model



A coupling electromechanical is created by the CP command and the appropriate voltage potential is assigned (Figure.7).

Figure.7. The electromechanical coupling

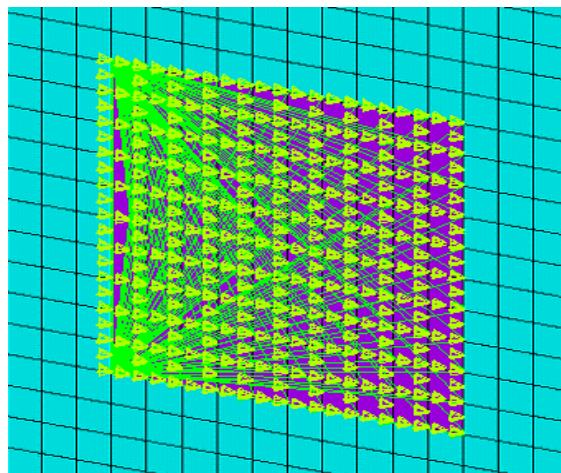
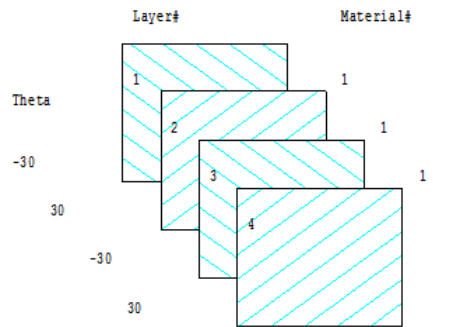


Figure 8 shows the four layers [-30/30/-30/30] of a composite plate, creating by **SECDATA** command.

Figure.8. Orientation of the ply in the composite plate



All simulations featured in this paper assume $\alpha = 0.5$ and $\beta = 0.025$ damping constants. In this approach. The smart composite plate in this case is exposed to a uniformly distributed load of 50 N/m^2 .

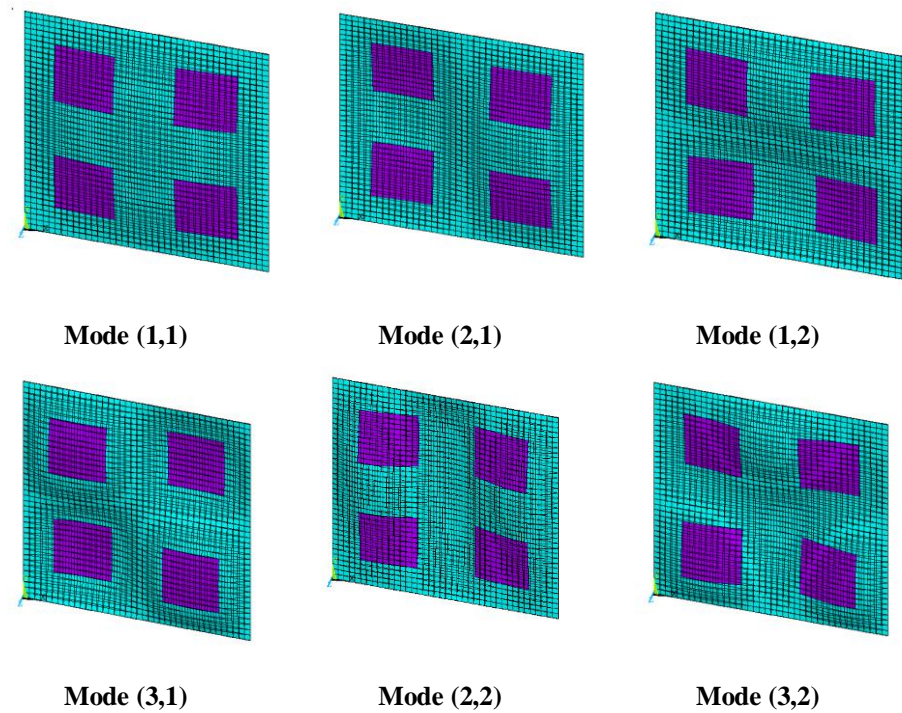
Steps are taken to identify the natural frequencies and mode shapes for the plate structures by using modal analysis. The time step Δt for Transient analysis is taken as $1/(20f_h)$, where f_h is the higher frequency. Consider an initial displacement field applied to the plate equal to 1 mm.

Table 2 shows the first six natural frequencies of the smart composite plate.

Table 2. The first six vibration modes of the smart composite plate

Modes (Rd/s)	(LIU[8])	ANSYS
Mode 1	174.573	175.102
Mode 2	354.818	354.612
Mode 3	481.046	497.514
Mode 4	637.596	640.351
Mode 5	688.55	700.254
Mode 6	935.439	1002.329

Figure 9 shows the first six vibration modes of the smart plate.

Figure.9. The six first vibration modes of the smart composite plate

The FEM results obtained by MATLAB software and valued by ANSYS APDL, to determine the cost function and the state space representation of the system. This model was obtained by system identification commands from MATLAB software using the frequency response of the smart plate.

In this study, a linear quadratic optimal controller is considered to control the first three modes of the flexible plate. The dynamic response is calculated using the first three modes. As a result, the size of system matrix $[A]$ is 6×6 . In addition, the size of the input matrix $[B]$ is 4×6 , the matrix $[B]$ depend of the number of actuators which four in our case.

Validation of the literature (G. Liu et al., 1999) are shown in Figure.10.

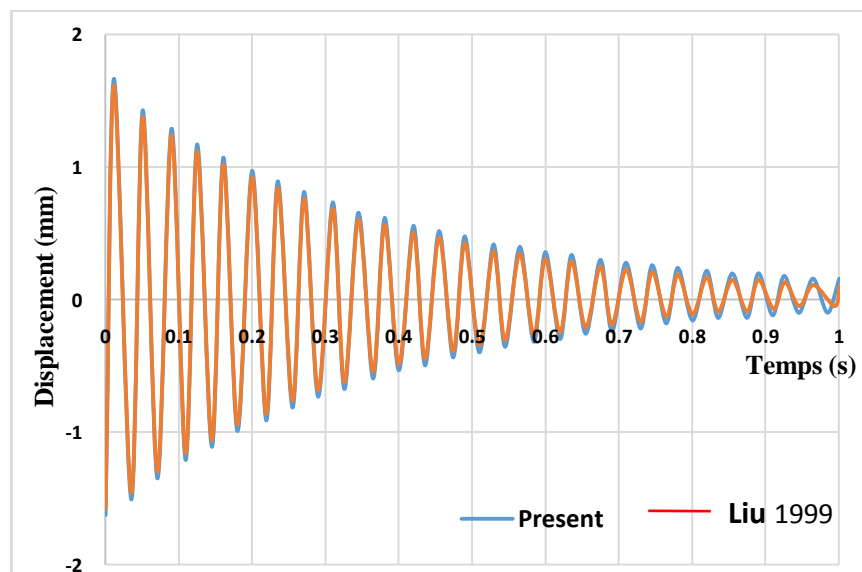
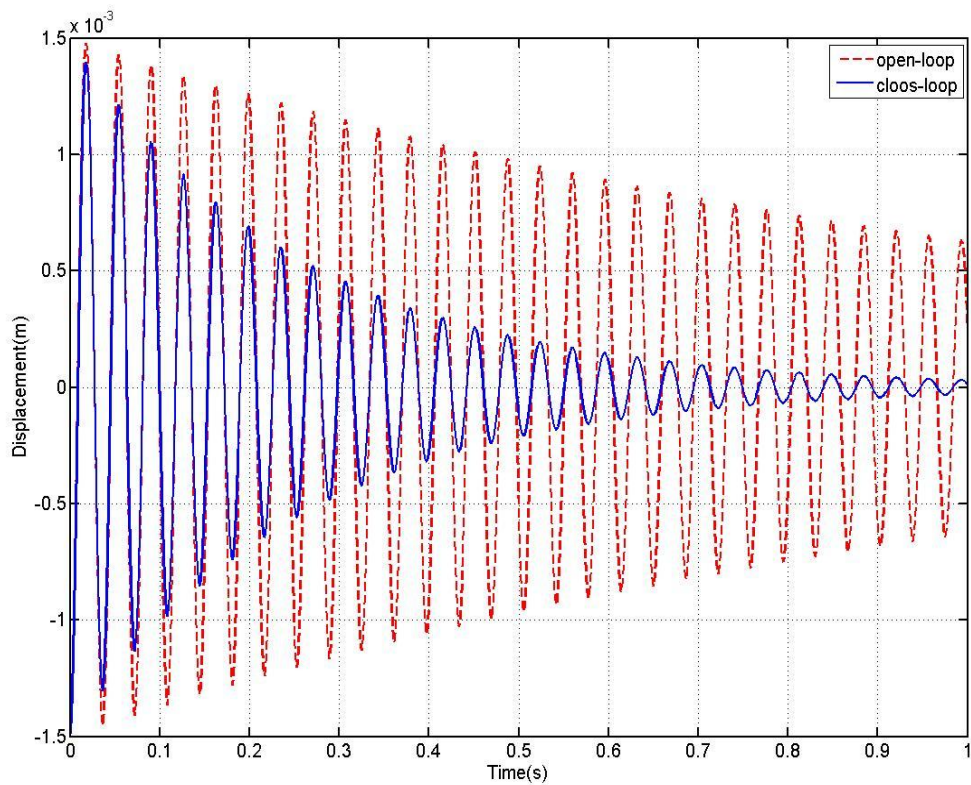
Figure.10. Validation of the literature (G. Liu et al., 1999)

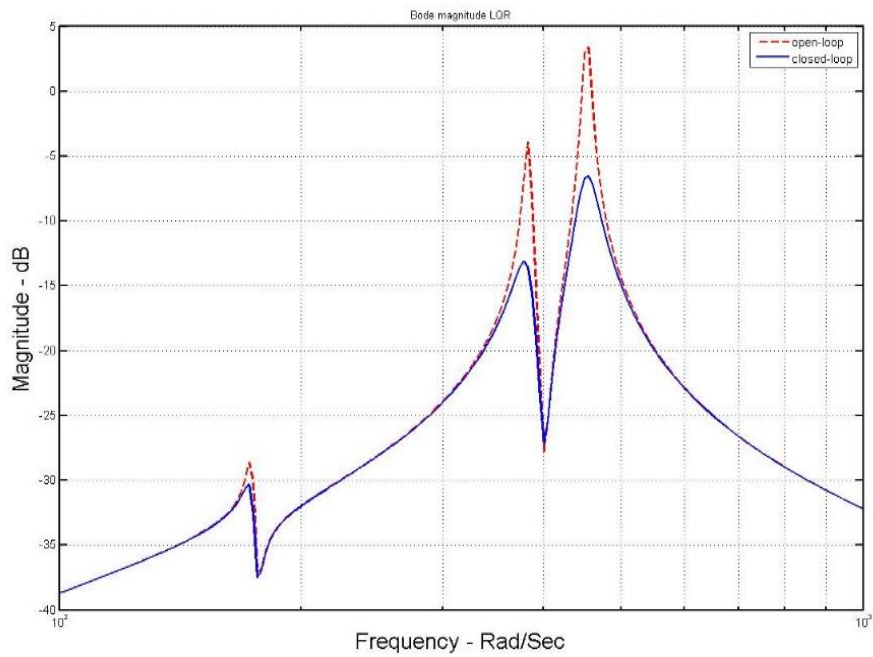
Figure 11 shows the displacement response of the smart composite plate in open and close loop.

Figure.11. The displacement response of the smart composite plate



The Bode plot of the open-loop and closed-loop system are shown in Figure.12, when the control is open-loop are also shown for comparison.

Figure.12. Frequencial response of the smart composite plate in M(0.2,0.2)



4.2. Active vibration control of the smart composite plate for different boundary conditions

In this section, the effect of the different boundary conditions in active vibration control is discussed. The previous smart composite plate is considered.

Table 3 shows the first six natural frequency of the smart composite plate for different boundary conditions. we denote by:

CCCC: Clamped- clamped- clamped- clamped ; CFCF: Clamped-free- clamped-free

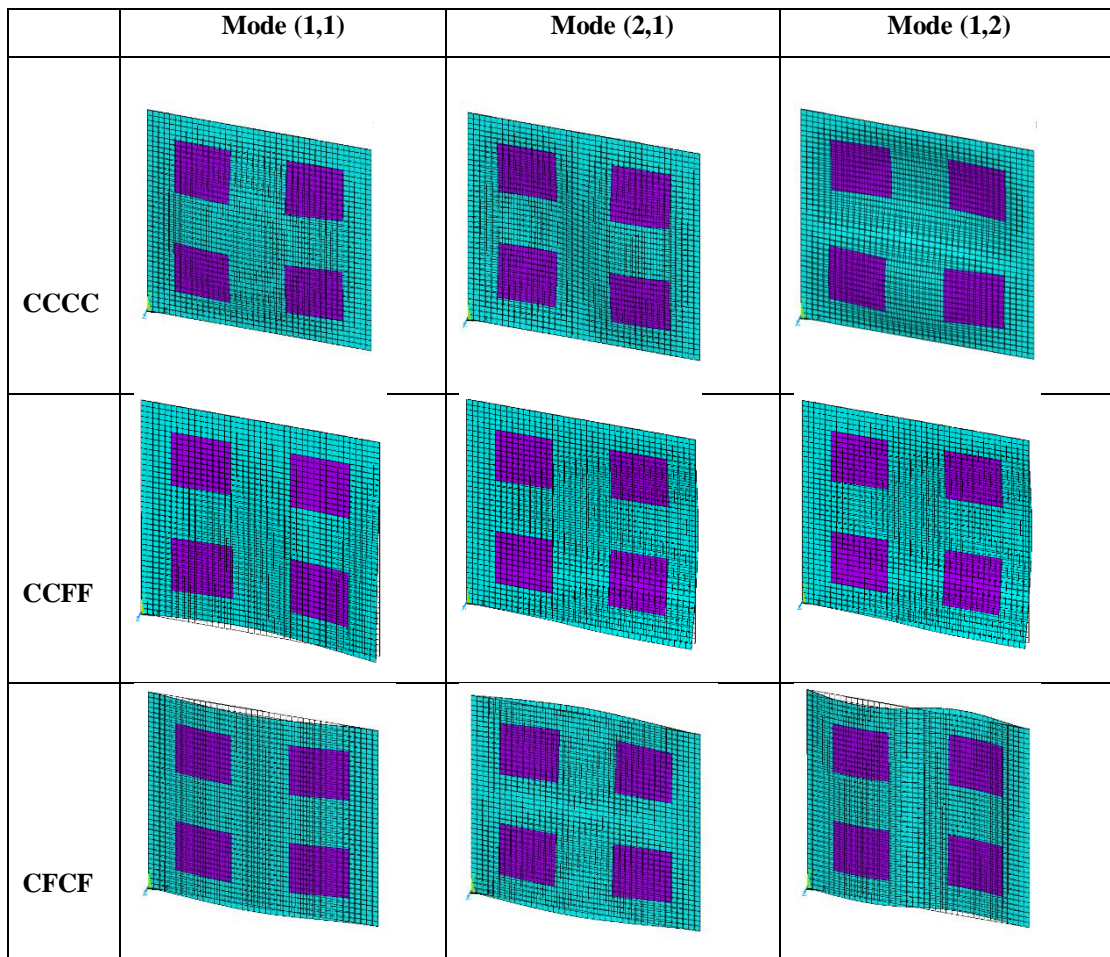
CCFF: Clamped- clamped-free-free ; CFFC: Clamped-free-free- clamped

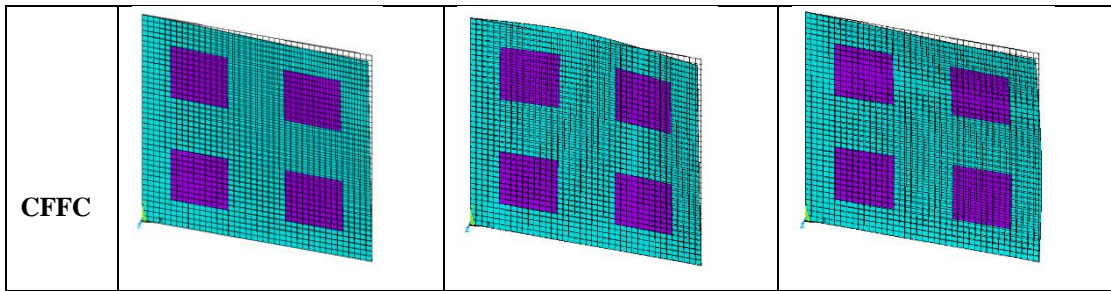
Table 3. The first six natural frequency of the smart composite plate for different boundary conditions

Modes (HZ)	CCCC	CCFF	CFCF	CFFC
Mode (2,1)	48.505	15.452	15.721	13.814
Mode (1,2)	76.072	33.021	35.798	24.298
Mode (3,1)	87.810	42.233	39.527	38.003
Mode (2,2)	91.056	45.381	44.549	40.646
Mode (3,2)	126.64	66.990	62.577	62.171

In figure13, the first three vibration modes of the smart composite plate for four conditions boundary are presented.

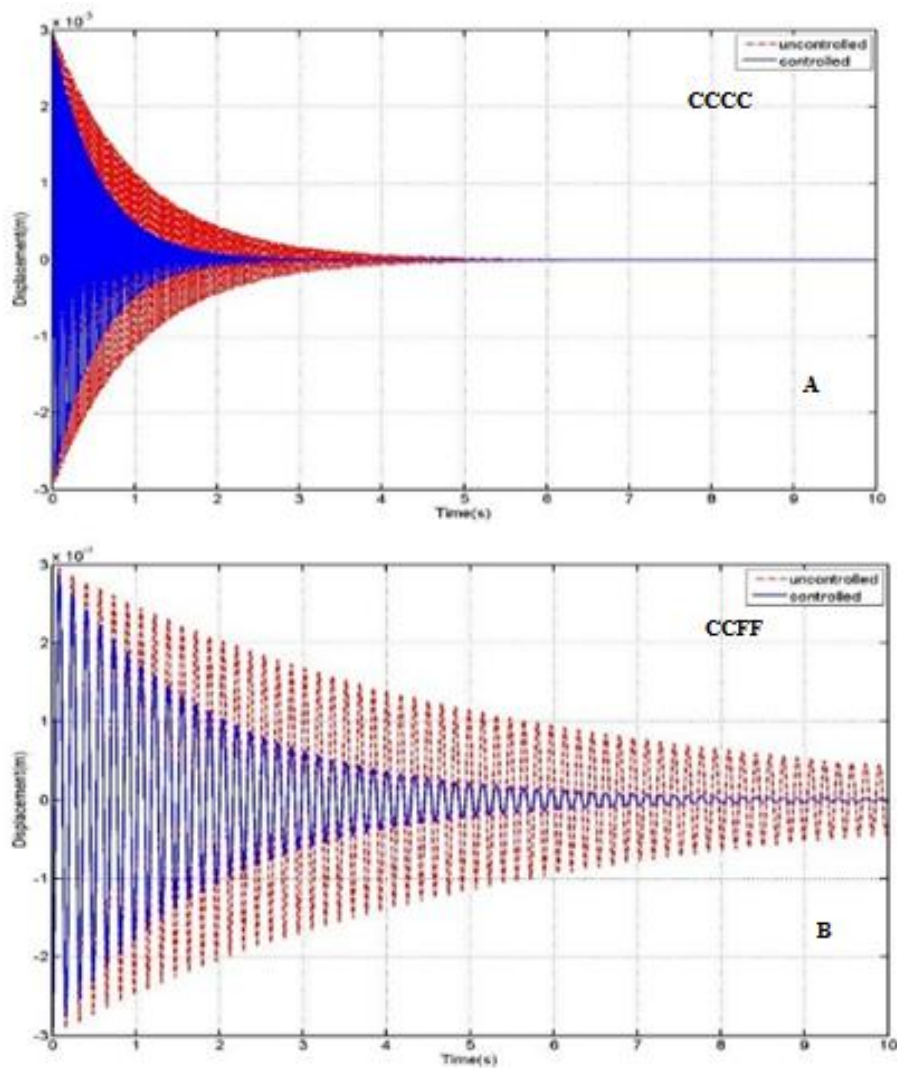
Figure.13. The three vibration modes of the smart composite plate for four different boundary conditions (CCCC, CCFF, CFCF, CFFC)

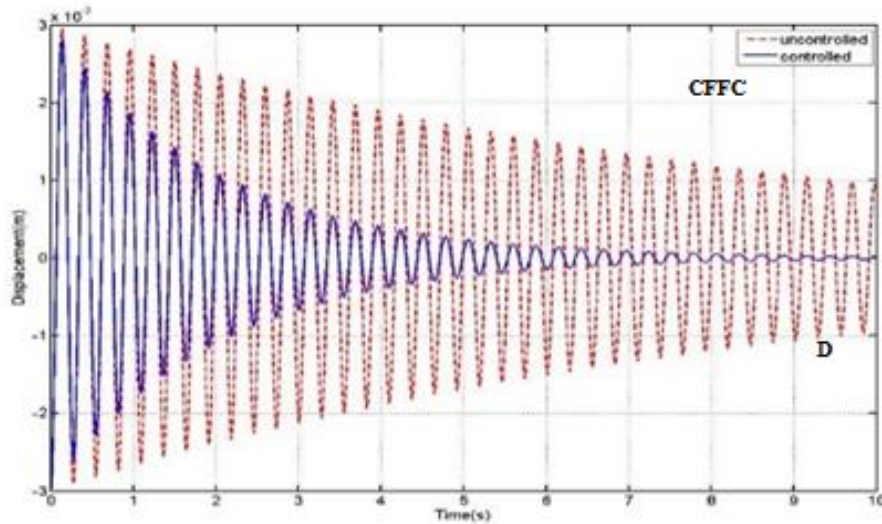
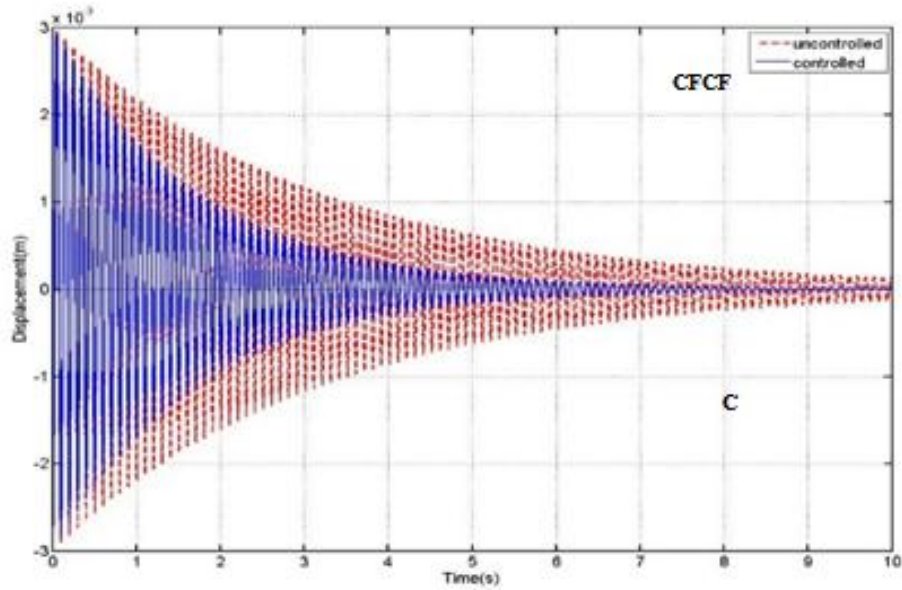




The displacements response of the plate in the point M (0.2,0.2) m and the Bode plot for four different boundary conditions (CCCC, CCFF, CFCF, CFCC) in close and open loop, are shown in Figure.14. and Figure.15 respectively.

Figure.14. The displasment response of the smart composite plate in M (0.2, 0.2) m for four boundary conditions (A, B, C, D).





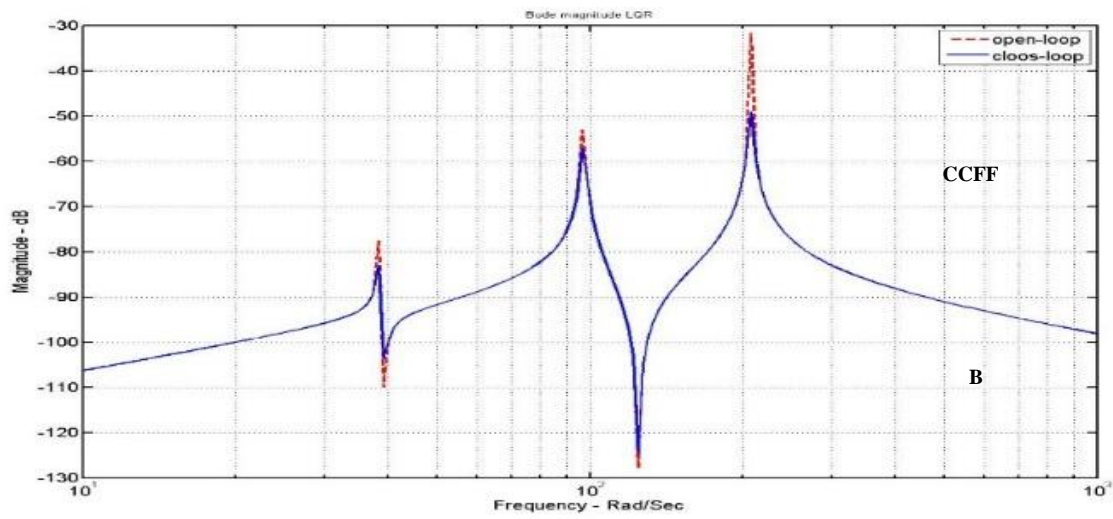
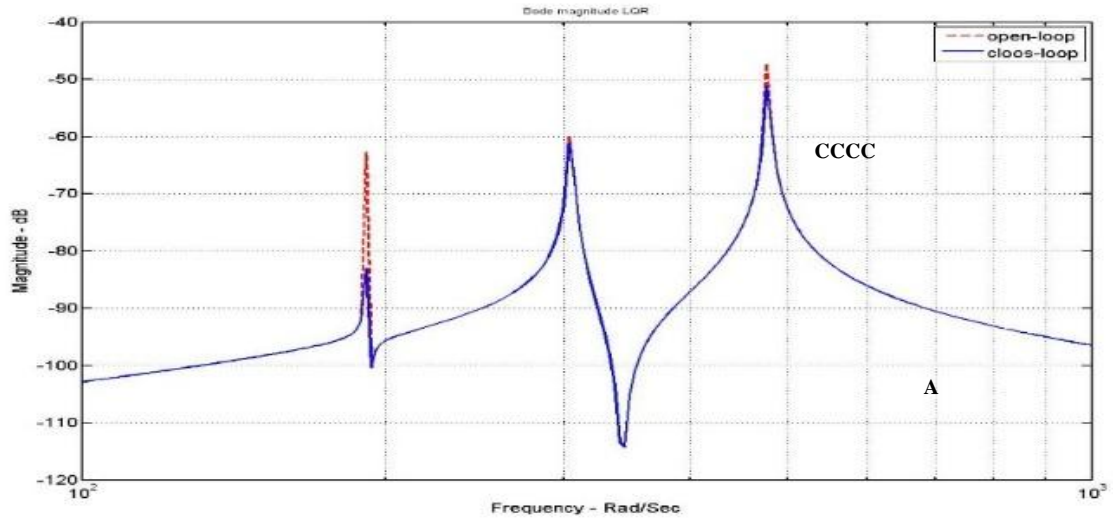
The different boundary conditions done different natural frequencies. The values matrix values A calculated by the first three natural frequencies. So, the transient response at the point $M(0.2,0.2)$ in each boundary condition (A, B, C and D) take a different form.

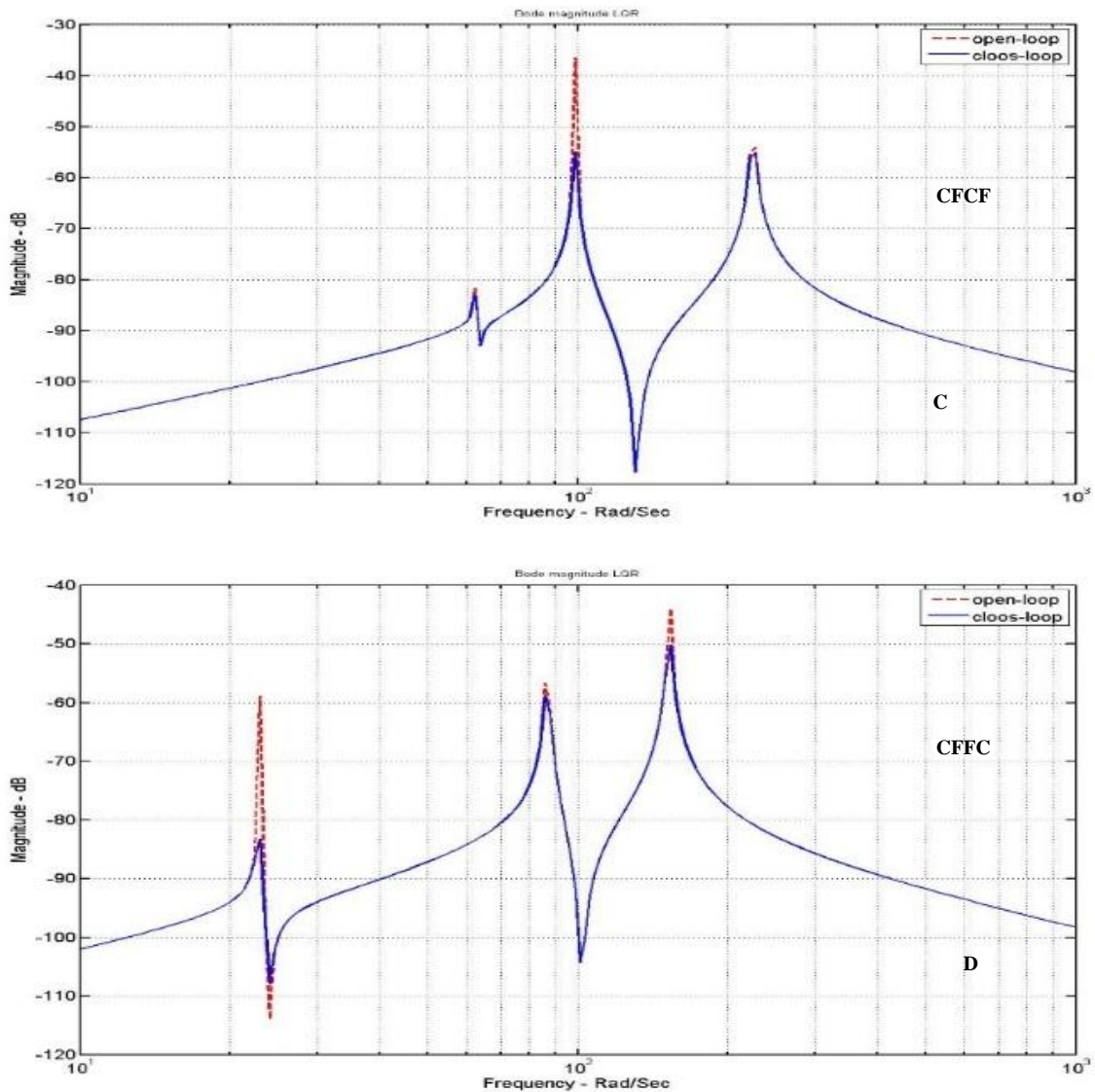
The shape of the curves of the Bode magnitude in the cases (A, B, C and D) are logically different, and the same thing with the curves (A, B, C and D) of the phase.

The active control of the smart composite plate is stable in the first five seconds for the case (CCCC). On the other cases, the other three cases (CCFF, CFCF, CFFC) stabilization is carried out within 10 seconds.

The boundary conditions of the controlled plate play a large role in the stabilization delay and the decrease value of the mode responses.

Figure. 15. The Bode plot response of the smart composite plate for four boundary conditions (A, B, C, D).





Conclusion

This paper proves the importance of using an appropriate FE model and an actually LQR perform the vibration control of piezoelectric composite plates.

With this work a procedure based on a finite element technique for solving a tow field coupling problem, such as the piezoelectric-structure interaction, is presented. We exploit the finite elements of software tool, ANSYS, for modelling the structure, and we exploit the software tool, MATLAB, for calculating control gains and simulating the system. The numerical results show the effectiveness of the procedure (LQR controller produces considerable reduction in both the settling time and the actuation force). The model is valued with the numerical results in literature. The damping tendencies of the various of boundary conditions of the smart composite plate have been found to be similar.

References

- Abdelrahman, W. G., Al-Garni, A. Z., Abdelmaksoud, S. I., & Abdallah, A. (2018). Effect of piezoelectric patch size and material on active vibration control of wind turbine blades. *Journal of Vibration Engineering & Technologies*, 6(2), 155-161.
- Biglar, M., Gromada, M., Stachowicz, F., & Trzepieciński, T. (2015). Optimal configuration of piezoelectric sensors and actuators for active vibration control of a plate using a genetic algorithm. *Acta Mechanica*, 226(10), 3451-3462.

- Cao, X., Tanner, G., & Chronopoulos, D. (2020). Active vibration control of thin constrained composite damping plates with double piezoelectric layers. *Wave Motion*, 92, 102423.
- Chandrashekhara, K., & Agarwal, A. (1993). Active vibration control of laminated composite plates using piezoelectric devices: a finite element approach. *Journal of intelligent material systems and structures*, 4(4), 496-508.
- Chhabra, D., Bhushan, G., & Chandna, P. (2016). Optimal placement of piezoelectric actuators on plate structures for active vibration control via modified control matrix and singular value decomposition approach using modified heuristic genetic algorithm. *Mechanics of advanced materials and structures*, 23(3), 272-280.
- Documentation, F. P. (2011). Release 12.1. *Ansys Inc.*
- Han, J.-H., & Lee, I. (1999). Optimal placement of piezoelectric sensors and actuators for vibration control of a composite plate using genetic algorithms. *Smart Materials and Structures*, 8(2), 257.
- Hasheminejad, S. M., & Oveisi, A. (2016). Active vibration control of an arbitrary thick smart cylindrical panel with optimally placed piezoelectric sensor/actuator pairs. *International Journal of Mechanics and Materials in Design*, 12(1), 1-16.
- Jandaghian, A., Jafari, A., & Rahmani, O. (2014). Vibrational response of functionally graded circular plate integrated with piezoelectric layers: An exact solution. *Engineering Solid Mechanics*, 2(2), 119-130.
- Jia, T., He, Q., & Zhang, R. (2020). *Study on linear quadratic regulator of high-speed elevator car horizontal vibration based on genetic algorithm optimization*. Paper presented at the International Conference on Maintenance Engineering.
- Kapuria, S., & Yasin, M. (2010). Active vibration suppression of multilayered plates integrated with piezoelectric fiber reinforced composites using an efficient finite element model. *Journal of Sound and Vibration*, 329(16), 3247-3265.
- Karegar, M., Bidgoli, M. R., & Mazaheri, H. (2021). *Smart control and seismic analysis of concrete frames with piezoelectric layer based on mathematical modelling and numerical method*. Paper presented at the Structures.
- Kumar, K. R., & Narayanan, S. (2007). The optimal location of piezoelectric actuators and sensors for vibration control of plates. *Smart Materials and Structures*, 16(6), 2680.
- Lee, C.-K., & Moon, F. C. (1990). Modal sensors/actuators.
- Liu, G., Peng, X., Lam, K., & Tani, J. (1999). Vibration control simulation of laminated composite plates with integrated piezoelectrics. *Journal of Sound and Vibration*, 220(5), 827-846.
- Liu, X., Cai, G., Peng, F., & Zhang, H. (2018). Piezoelectric actuator placement optimization and active vibration control of a membrane structure. *Acta Mechanica Solida Sinica*, 31(1), 66-79.
- Malgaca, L. (2010). Integration of active vibration control methods with finite element models of smart laminated composite structures. *Composite Structures*, 92(7), 1651-1663.
- Mallek, H., Jrad, H., Wali, M., & Dammak, F. (2021). Nonlinear dynamic analysis of piezoelectric-bonded FG-CNTR composite structures using an improved FSDT theory. *Engineering with Computers*, 37(2), 1389-1407.
- Quek, S., Wang, S., & Ang, K. (2003). Vibration control of composite plates via optimal placement of piezoelectric patches. *Journal of intelligent material systems and structures*, 14(4-5), 229-245.
- Reddy, J. N. (1984). A simple higher-order theory for laminated composite plates.
- Reddy, J. N. (2003). *Mechanics of laminated composite plates and shells: theory and analysis*: CRC press.
- Roy, T., & Chakraborty, D. (2009). Genetic algorithm based optimal design for vibration control of composite shell structures using piezoelectric sensors and actuators. *International Journal of Mechanics and Materials in Design*, 5(1), 45-60.
- Sadri, A., Wright, J., & Wynne, R. (1999). Modelling and optimal placement of piezoelectric actuators in isotropic plates using genetic algorithms. *Smart Materials and Structures*, 8(4), 490.
- Schulz, S. L., Gomes, H. M., & Awruch, A. M. (2013). Optimal discrete piezoelectric patch allocation on composite structures for vibration control based on GA and modal LQR. *Computers & Structures*, 128, 101-115.
- Sethi, V., & Song, G. (2004). *Multimode optimal vibration control of flexible structure using piezoceramics*. Paper presented at the Proceedings of the 2004 IEEE International Symposium on Intelligent Control, 2004.
- Sohn, J. W., Choi, S.-B., & Kim, H. S. (2011). Vibration control of smart hull structure with optimally placed piezoelectric composite actuators. *International Journal of Mechanical Sciences*, 53(8), 647-659.
- Tian, J., Guo, Q., & Shi, G. (2020). Laminated piezoelectric beam element for dynamic analysis of piezolaminated smart beams and GA-based LQR active vibration control. *Composite Structures*, 252, 112480.
- Wankhade, R., & Bajoria, K. (2021). Vibration attenuation and dynamic control of piezolaminated plates for sensing and actuating applications. *Archive of Applied Mechanics*, 91(1), 411-426.